Prostate Imaging and Interventions at 0.55T: Increasing Access to High-Quality Prostate Cancer Diagnosis and Treatment

Joseph Busch, Jr., M.D.

Founder, Busch Center, Alpharetta, GA, USA

Introduction

Magnetic resonance imaging (MRI) of the prostate has become an integral part of the standard of care for prostate cancer management, supported by multiple randomized trials demonstrating superiority of MRI-targeted over systematic biopsy for clinically significant prostate cancer detection [1]. A growing body of evidence also supports the role of MRI to guide active surveillance of favorable-risk prostate cancer [2], post-treatment follow-up and recurrence evaluation [3–5], and even population-level prostate cancer screening [6]. In parallel, advances in interventional MRI (iMRI) have expanded the role of prostate MRI beyond diagnostic imaging to encompass image-guided interventions like in-bore MRI-guided biopsy as well as intraoperative treatment planning and real-time treatment monitoring [7] (Fig. 1). The increasingly central role of MRI across the prostate cancer care continuum underscores the need to achieve reproducible outcomes beyond academic centers, and to broaden access to high-quality prostate MRI and MRI-guided procedures.

Access to high-quality prostate MRI is limited due to the high prevalence of suboptimal imaging protocols even among expert sites, and due to the high cost of traditional high-field MRI, which is not available widely enough to serve the expanding population of patients for whom prostate MRI is indicated. This has stimulated initiatives to standardize prostate MRI acquisition and interpretation, and has driven interest in lower-field MRI systems, where recent advances have enabled high-quality imaging with potential advantages in accessibility and workflow integration. Moreover, the inherent characteristics of low-field MRI reduce susceptibility artifacts, enhance patient access, and lower operating costs, making it particularly well-suited for interventional applications. Here we review drivers of prostate MRI quality, which recent studies suggest are mostly practical matters that are independent of MRI field strength. We also discuss how technological developments that enable high-performance imaging on lower-field scanners could enable broader access to diagnostic and interventional MRI, and we evaluate the feasibility of prostate MRI and interventions at 0.55T.

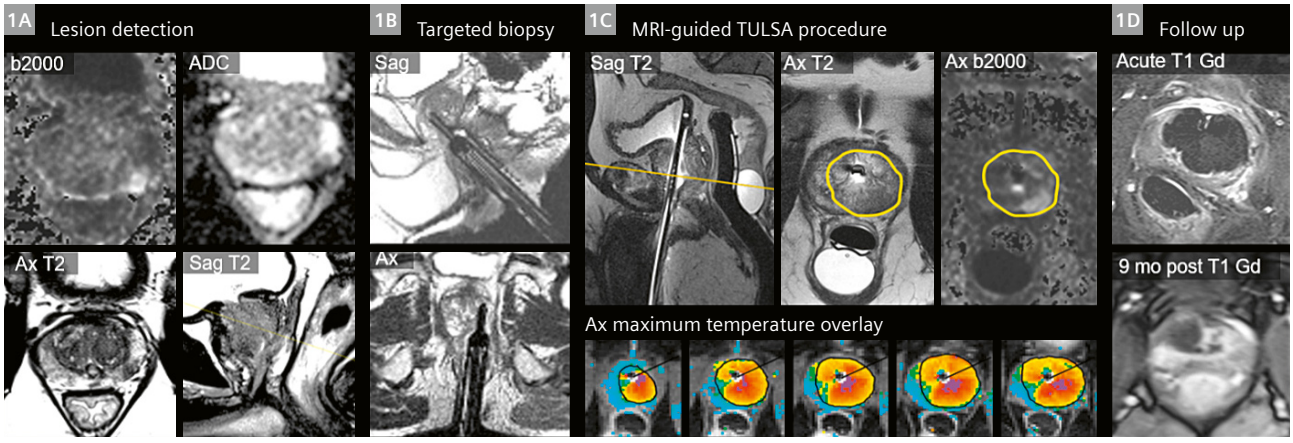

1 The role of MRI from prostate cancer diagnosis to treatment and follow-up, currently performed and demonstrated here at 1.5T and 3T. **(1A)** Diffusion and T2-weighted images enabling lesion detection, localization, and staging. **(1B)** In-bore MRI-targeted biopsy for accurate sampling of MRI-visible lesions. **(1C)** MRI-guided ablation with TULSA including intraoperative T2- and diffusion-weighted planning, and real-time MR thermometry used for automated treatment control to achieve the intended ablation volume. **(1D)** Post-treatment contrast-enhanced MRI to evaluate the acute ablation zone and follow treatment response.

Drivers of prostate MRI quality

As Level 1 evidence on MRI-directed prostate cancer management has accumulated, MRI before prostate biopsy is now firmly established as the standard of care in international practice guidelines. With rising demand for prostate MRI, concerns have increased about the ability to reproduce clinical trial results outside specialized academic centers, and international guidelines caution that the utility of prostate MRI in the diagnosis of prostate cancer depends critically on the quality of image acquisition and interpretation [8]. This has prompted efforts to study variability in the diagnostic performance of prostate MRI, to establish standards for the assessment of prostate MRI quality, and to systematically improve the quality of prostate MRI programs.

One of the largest efforts to study the consistency of prostate MRI performance, conducted by the Society for Abdominal Radiology Prostate Cancer Disease-Focused Panel, found that even leading academic centers have difficulty achieving high-quality diagnostic prostate MRI [9]. In more than 3,000 men at 26 premier academic centers, more than half of the sites had a rate below 50% for correctly identifying clinically significant prostate cancer, with a positive predictive value of less than 0.5 for lesions with a PI-RADS (Prostate Imaging and Reporting and Data System) score of 4 or higher. Interestingly, the wide variability across centers did not appear to depend on the use of 1.5T versus 3T scanners; instead, the leading causes of poor-quality prostate MRI were typically practical concerns related to scan protocol and patient preparation, including the management of rectal gas. In the UK PRIME trial [10], which assessed and established standards for prostate MRI quality at 41 centers across 18 countries using the Prostate Imaging Quality (PI-QUAL) scoring system, only 32% of submitted test exams demonstrated optimal image quality (PI-QUAL score 5 out of 5). In that study, the leading reasons for suboptimal PI-QUAL scores included basic protocol errors such as inadequate resolution, field of view, slice thickness, diffusion b-values, temporal resolution of dynamic contrast-enhanced images, motion artifacts, and air in the rectum. With feedback from the central quality-improvement group about making simple changes to MRI protocols and patient preparation, 97% of participating centers achieved optimal PI-QUAL 5 scores upon repeat assessment. Similarly, the American College of Radiology's Prostate MR Image Quality Improvement Collaborative followed PI-QUAL scores across 2,380 exams over 9 months at 5 large hospital networks [11]. They found that the rate of diagnostic-quality exams improved from 67% to 87% through protocol adjustments, specifically the consistent application of clear patient preparation instructions (including prompts to use the bathroom before the exam, and at some centers the use of a mini enema), MRI technologist training, and periodic review of diagnostic performance with feedback to MRI technologists and radiologists [11]. Across these and other quality-improvement studies, key drivers of improved prostate MRI quality tended to be practical interventions rather than movement to higher field strength.

At the Busch Center, which focuses entirely on prostate MRI and MRI-guided interventions, prostate MRI examinations begin with consistent patient preparation performed in-office using a mini enema immediately before the exam in a dedicated bathroom for pre-exam preparation. An essential aspect of the MRI protocol is performing the diffusion scan first, as this sequence is most sensitive to patient motion and bowel gas, both of which are more likely to arise as time goes on. If motion or rectal air artifacts do appear, the examination is paused and the patient is asked to repeat the mini enema before continuing. Finally, the overall diagnostic quality of the study depends on the quality of interpretation; radiologists are encouraged to invest in training and mentorship, specialize in reading prostate MRI examinations, and continuously review biopsy reports based on MRI targeting to improve accuracy and to understand the relationship between histologic grade and apparent diffusion coefficient (ADC) values on their machine [12].

Accordingly, technology improvements to raise the quality of prostate MRI are ideally focused on ensuring consistent application of best practices in image acquisition and diagnosis. There has been significant development in the standardization of streamlined acquisition protocols, with results from the PRIME study confirming that simplified biparametric protocols comprised only of T2 and high-b diffusion-weighted imaging (DWI) did not reduce cancer detection compared to multiparametric prostate MRI protocols including time-consuming and highly variable dynamic contrast-enhanced (DCE) T1-weighted acquisitions [13]. MRI vendors are developing AI tools that assist technologists in improving the consistency of prostate MRI acquisition with automated slice prescription, that shorten acquisition times and thus motion artifacts without reducing the signal-to-noise ratio (SNR) using AI-powered image reconstruction and post-processing techniques (Deep Resolve), and that automatically identify image artifacts and notify technologists to repeat scans while patients are still in the scanner [14]. Numerous tools are also being developed to assist radiologists in evaluating prostate MRI, with automated segmentation of the prostate gland and zonal anatomy, machine learning-based lesion detection and grading validated against biopsy or whole-mount histology to improve diagnostic yield for less experienced readers, and auto-population of imaging reports to ensure adherence to established standards such as PI-RADS, PRECISE, and PI-RR (AI-Rad Companion). Together, these improvements have the potential to not only maintain, but also improve the quality and consistency of prostate MRI as the number of programs and cases increases.

0.55T: Increasing access to high-quality prostate MRI

While demand for prostate MRI is increasing, and the combination of protocol standardization and technological improvements is raising the ability of new programs to achieve high diagnostic yield, there are also significant economic and geographic disparities in access to MRI [15]. Compared with traditional high-field magnets, helium-free scanners reduce the complexity of MRI installation, enabling deployment of imaging capabilities to previously inaccessible locations while also significantly decreasing the cost of acquisition, buildout, and operation, thereby reducing barriers to entry. Helium-free scanners with ultra-wide 80 cm bores also increase access by supporting imaging of bariatric and claustrophobic patients. Furthermore, imaging at 0.55T instead of higher fields lowers barriers for patients with metal implants by decreasing SAR-induced heating and reducing susceptibility artifacts around implants, and may also improve reproducibility by decreasing the susceptibility-related effects of air in the rectum.

While there are numerous potential advantages to prostate imaging with a modern 0.55T scanner, it is not yet known whether improvements in hardware and AI-enhanced reconstruction can overcome the lower SNR relative to higher field strengths to produce diagnostic-quality T2 and diffusion-weighted images. The current PI-RADS guidelines for reporting prostate MRI advise against prostate imaging below 1.5T because of limited experience and limited prospective assessment of diagnostic performance at lower field strengths. To date, publications on prostate MRI at 0.55T have focused on protocol development [16], technical analysis of anatomical features compared with 1.5T and 3T [17], and guidance of in-bore MRI-targeted biopsy [18]. Evaluations of diagnostic performance at 0.55T or diagnostic comparisons with higher field strengths are not yet available.

To explore the feasibility of prostate imaging using ultrawide-bore, helium-free 0.55T MRI, we ported our 3T MAGNETOM Skyra biparametric prostate MRI protocol to the MAGNETOM Free.Max system for volunteer imaging in a series of three participants at the MRI facility of Siemens Healthineers in Erlangen, Germany. Table 1 lists the technical scan parameters that have quality specifications in the PI-RADS reporting guidelines. Without optimization, this initial attempt at volunteer imaging met all PI-RADS technical specifications (except field of view on the diffusion scan, which was later updated with minimal change in

Sequence	PI-RADS technical specification	3T MAGNETOM Vida protocol	0.55T MAGNETOM Free.Max protocol
Axial T2W			
Slice thickness (mm)	3, no gap	3, no gap	3, no gap
Field of view (cm)	12–20	20	20
In-plane dimension (mm)	≤ 0.7 (phase), ≤ 0.4 (frequency)	0.3 × 0.3	0.4 × 0.4
Echo train length	Excessive ETL to be avoided	51	27
Acquisition duration (min:sec)	–	1:14	3:10
Axial DWI			
Echo time (ms)	≤ 90	63	89
Repetition time (ms)	≥ 3000	3800	4300
Slice thickness (mm)	≤ 4, no gap	3	3
Field of view (cm)	16–22	20	24
In-plane dimension (mm)	≤ 2.5 phase & frequency	0.9 × 0.9	1.3 × 1.3
Low b-value (s/mm^2)	0–100 (preferably 50–100)	50	50
Intermediate b-value (s/mm^2)	800–1000	800	800
High b-value (s/mm^2)	≥1400 (separate or calculated)	calc b2000	calc b1400
Acquisition duration (min:sec)	–	1:56	5:18

Table 1: Comparison of sequence parameters used for volunteer imaging at 0.55T.

image quality or scan time). Despite a nearly sixfold decrease in magnetic field strength, PI-RADS-compliant scans were attainable with a modest increase in scan time.

The first volunteer (Fig. 2) was a man in his 80s with a prostate volume of approximately 100 cc. In addition to axial T2-weighted and diffusion scans, the test protocol also included sagittal, coronal, and 3D T2W acquisitions. The T2-weighted images met all criteria for diagnostic quality by satisfying the PI-RADS and PI-QUAL technical specifications, including axial and orthogonal views, clear delineation of the capsule, seminal vesicles, ejaculatory ducts, neurovascular bundles, and sphincter muscle, and freedom from motion or rectal air artifacts. The DWI sequence was free of rectal air artifacts, with surprisingly high SNR, resolution, and geometric fidelity in ADC maps and calculated b2000 images. A small focus in the transition zone was clearly visible, with hypointensity on T2W, high signal intensity indicating restricted diffusion on high-b DWI, and low ADC values of 600–800 sec/mm^2. Given the transition-zone location, this was consistent with a PI-RADS 4 lesion and likely low histologic grade.

The second volunteer, a man in his 60s with a 40 cc gland, also demonstrated excellent depiction of the intra- and extraprostatic anatomy (Fig. 3). A focus of hyperintensity was seen in the right anterior transition zone on the calculated b1400 images, but the corresponding ADC values were above 900 × 10^{-6} mm^2/s and the finding lacked conspicuity on T2W images. The combined T2-weighted, diffusion-weighted, and susceptibility-weighted images demonstrated the feasibility of acquiring high-quality anatomical and functional prostate MRI at 0.55T.

The third volunteer, a 50-year-old man with an approximately 40 cc prostate and no history of prostate cancer, was imaged at both 0.55T and 3T on the same day (Fig. 4). Anatomical contrast and resolution on T2W images were effectively equivalent for the detection of clinically significant lesions. DWI resolution and contrast were superior at 3T, but clear visualization of the transition zone and peripheral zone, together with concordant conspicuity of a focus of restricted diffusion in the right transition zone, speak to the potential for diagnostic prostate MRI at 0.55T.

Prostate interventions at 0.55T: Transurethral ultrasound ablation (TULSA)

As described in several articles in this issue, ultra-wide-bore, 0.55T, almost helium-free magnets offer numerous technical and practical advantages for MRI-guided interventions. The wider bore facilitates interventional device insertion and manipulation, the lower field reduces device-associated image artifacts and heating concerns, and helium-free operation reduces cost, making it feasible for private-practice surgeons and interventionalists to establish their own MRI-guided interventional suites.

One of the most mature technologies for in-bore MRI-guided prostate ablation is transurethral ultrasound ablation (TULSA). Each single-use TULSA ultrasound applicator (UA) uses a linear array of 10 directional ultrasound

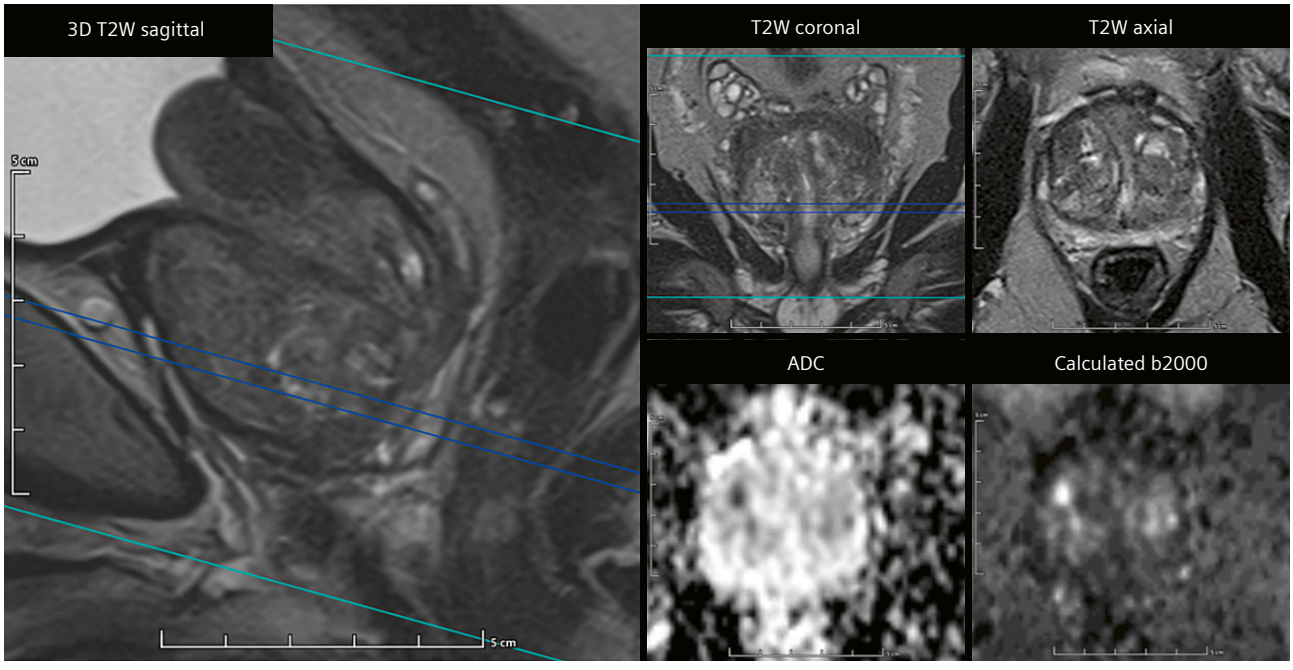

2 Prostate MRI in an 83-year-old healthy volunteer on a 0.55T MAGNETOM Free.Max system. Representative images include T2-weighted images in sagittal, coronal, and axial planes, along with axial apparent diffusion coefficient (ADC) and high calculated b-value diffusion-weighted (b = 2000 s/mm^2) images, demonstrating prostate visualization and image quality at low field strength.

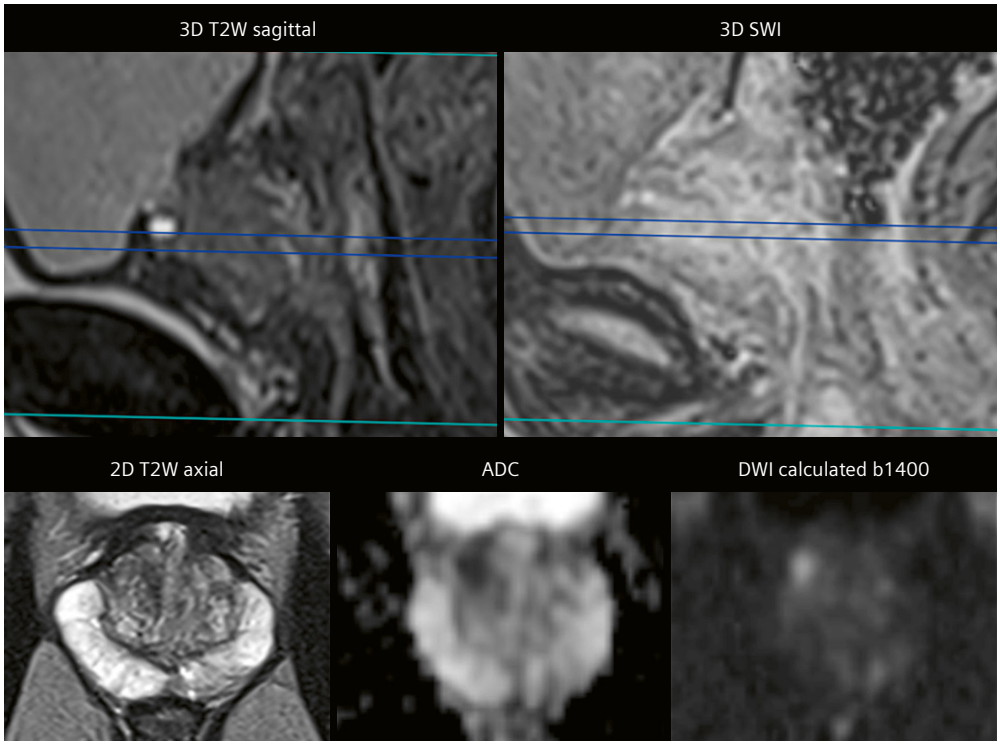

3 Prostate MRI from a 64-year-old healthy volunteer acquired using the 0.55T MAGNETOM Free.Max. The top row shows a 3D T2-weighted sagittal image (left) and a 3D sagittal susceptibility-weighted imaging (SWI) acquisition (right; in-plane resolution 0.65 × 0.65 mm^2, slice thickness 2 mm). The bottom row shows the corresponding axial T2-weighted image, apparent diffusion coefficient (ADC) map, and high b-value (b = 1400 s/mm^2) diffusion-weighted image (DWI). The blue reference line displayed on the sagittal images indicates the location of the axial slice shown in the bottom row.

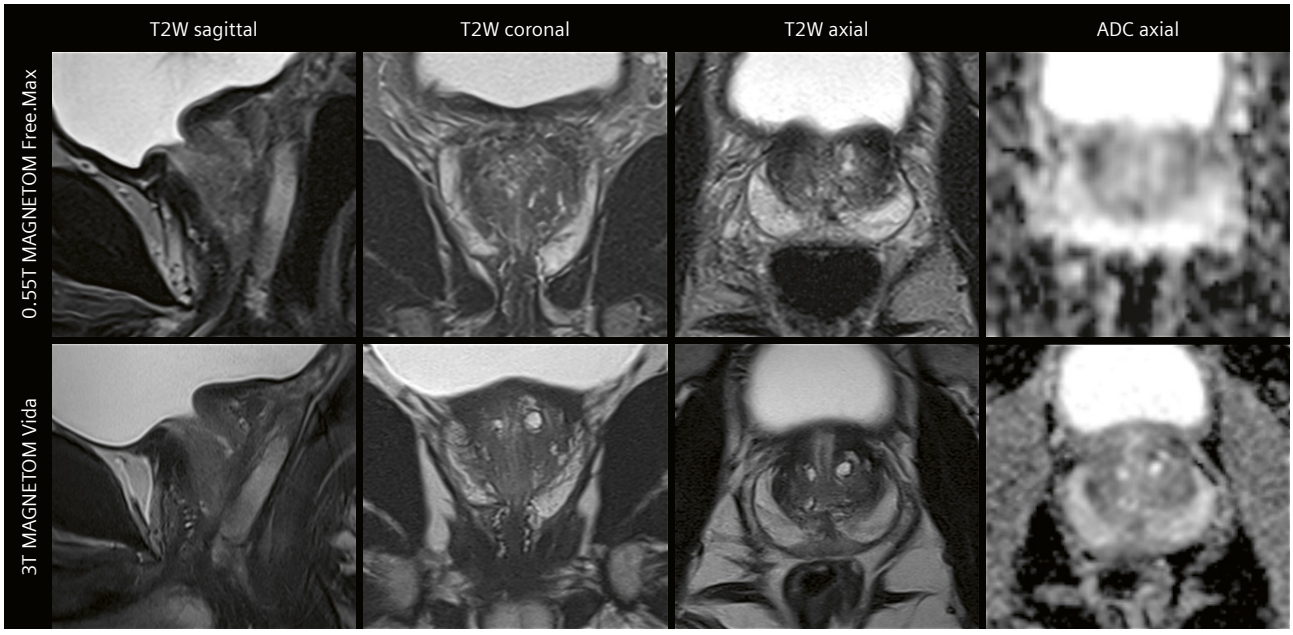

4 Multiplanar T2- and diffusion-weighted prostate MRI in a 50-year-old man at 0.55T and 3T. Sagittal, coronal, and axial images are shown for comparison between a 0.55T system (MAGNETOM Free.Max) (top row) and a 3T system (MAGNETOM Vida) (bottom row). Both scans were acquired on the same day. The 3T examination demonstrates greater bladder distension at the time of imaging. Despite differences in field strength, corresponding anatomical structures are consistently visualized across all planes, demonstrating feasibility of low-field imaging for prostate MRI.

beams to form a "blade" of energy that achieves thermal coagulation of prostate tissue extending from the urethra to the prostatic capsule. An MRI-compatible robot automates precise image-guided positioning of the applicator during planning, and continuous computer-controlled rotation of the ultrasound blade during treatment. Historically performed at 1.5T and 3T, TULSA leverages the superior soft tissue contrast of MRI for accurate lesion localization and target delineation. It also harnesses MRI's unique capability to achieve fast, high-precision, volumetric temperature mapping to monitor and provide quantitative feedback control that drives thousands of automatic adjustments of ultrasound power and penetration depth for conformal thermal ablation of targeted prostate tissue with millimeter precision while preserving surrounding healthy tissue and functional outcomes. The MRI-guided transurethral approach to thermal energy delivery has demonstrated decreased morbidity, promising efficacy, and broad treatment flexibility for focal and whole-gland ablation across the spectrum of prostate disease, including in early feasibility studies [19–21], a pivotal multicenter trial in localized prostate cancer [22, 23], and investigator-initiated studies in radio-recurrent prostate cancer [24] as well as tissue debulking for benign prostatic hyperplasia (BPH) [25]. A multicenter randomized controlled trial comparing TULSA to robotic prostatectomy (CAPTAIN, NCT05027477) has completed enrollment, with early outcomes demonstrating superior safety and quality-of-life for TULSA [26]; oncologic outcomes will be reported at 3 and 10 years.

During TULSA treatment, standard diagnostic 3 mm axial T2-weighted and diffusion-weighted images such as those evaluated at 0.55T in the volunteers above are acquired to delineate the planned ablation volume with visualization and sparing of neurovascular bundles, urethra, sphincter complex, and adjacent critical structures. Additionally, 3D T2-weighted imaging with 1 mm isotropic voxels is particularly valuable to delineate the prostatic apex and external urinary sphincter for preservation of urinary function in patients with apical lesions [27]. Figure 5 shows high-resolution isotropic 3D T2-weighted imaging at 0.55T from the second volunteer, demonstrating clear visualization of the prostate zonal anatomy

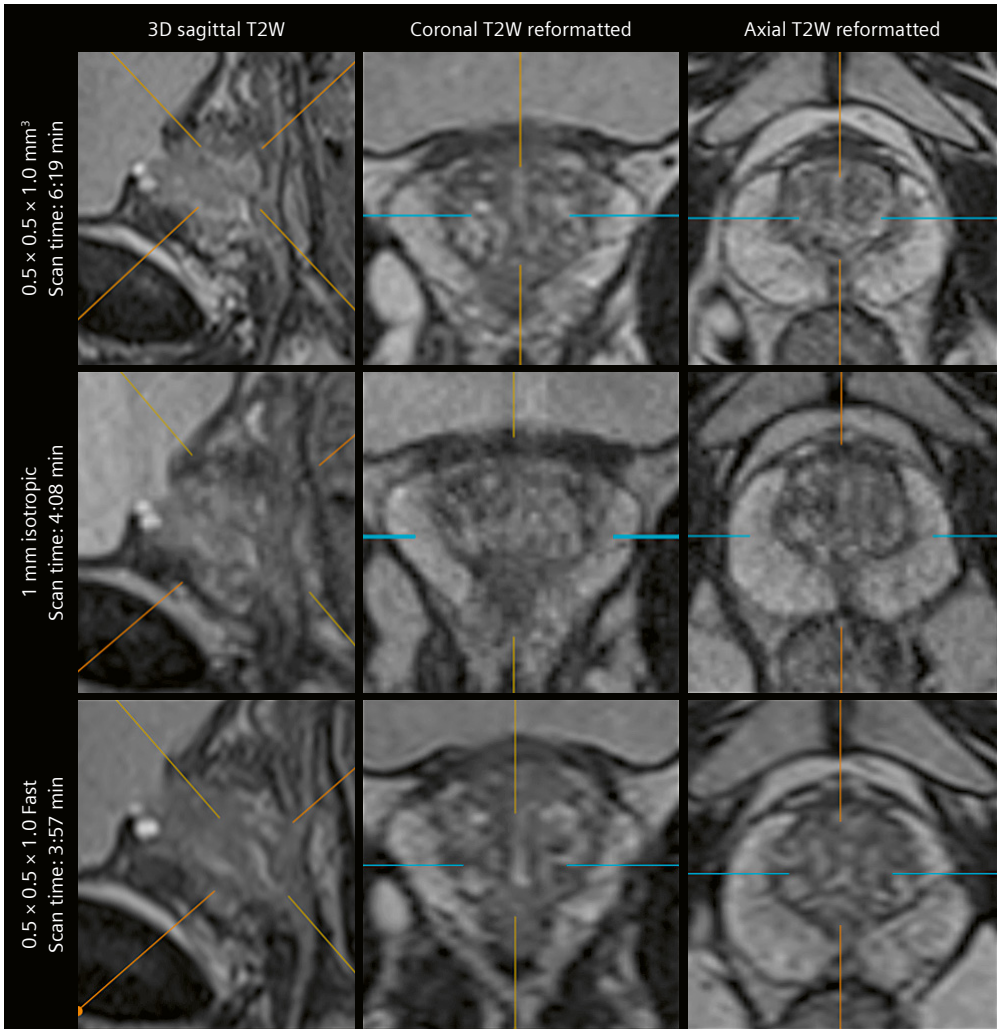

5 Representative prostate MRI from a 64-year-old healthy volunteer acquired on a 0.55T MAGNETOM Free.Max system. Rows (top to bottom) show images from T2 SPACE sag (acquisition time 6:19 min; voxel size 0.5 × 0.5 × 1.0 mm³), T2 SPACE sag (acquisition time 4:08 min; isotropic voxel size 1.0 × 1.0 × 1.0 mm³), and T2 sag fast (acquisition time 3:57 min; voxel size 0.5 × 0.5 × 1.0 mm³). Columns (left to right) display the original 3D sagittal T2-weighted acquisition, coronal reformat, and axial reformat, respectively. All acquisitions were obtained with a slice thickness of 1 mm.

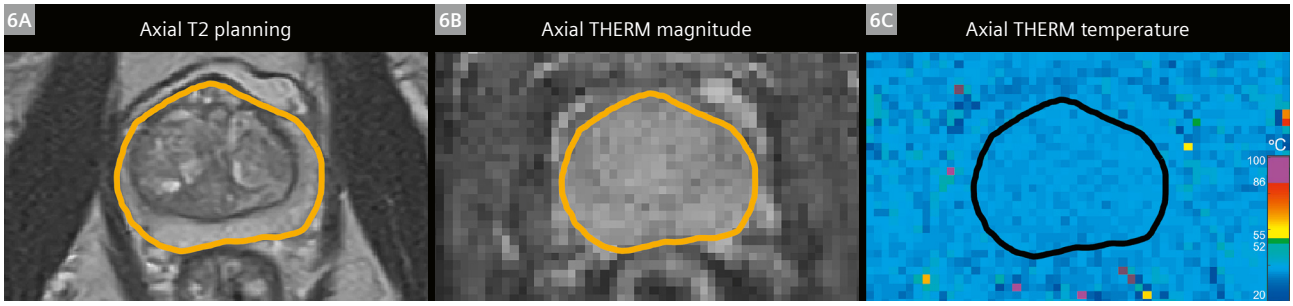

6 Three-dimensional MR thermometry for MRI-guided TULSA therapy at 0.55T. **(6A)** Axial T2-weighted treatment planning image. **(6B)** Axial thermometry magnitude image acquired during treatment. **(6C)** Corresponding axial temperature map demonstrating stable real-time thermal monitoring.

and surrounding pelvic structures in sagittal, coronal, and axial reconstructions.

The most critical consideration for TULSA at lower field strengths with lower overall signal-to-noise ratio is maintaining the accuracy of MRI temperature monitoring needed for precise ablation control. To address the anticipated decrease in SNR at lower field, a 3D MR thermometry sequence was implemented at 0.55T in place of conventional 2D acquisitions, enabling equivalent temperature monitoring resolution, coverage, and speed, while improving SNR efficiency (Fig. 6). Technical validation of the MAGNETOM Free.Max TULSA-PRO platform demonstrated that the precision of 3D thermometry at 0.55T was comparable to that achieved with standard 2D thermometry at 1.5T while maintaining the same scan time, voxel size, and field-of-view. These findings suggest that the MAGNETOM Free.Max can support real-time visualization and control of thermal deposition during MRI-guided prostate ablation with TULSA, while maintaining temperature measurement precision and enabling the workflow, accessibility, and cost advantages associated with lower-field systems.

Outlook and perspective

With widespread adoption of MRI in prostate cancer diagnosis and management, it is important to be aware of the practical steps that can be taken to ensure high diagnostic performance of prostate MRI programs. High-quality prostate MRI is achieved by paying careful attention to consistent patient preparation, standardized MRI protocols, technologist training, and feedback among technologists, radiologists, and pathologists. Low-field, wider-bore, helium-free MRI scanners such as the MAGNETOM Free.Max have the potential to increase access to prostate MR imaging and interventions due to broadened patient eligibility and the lower technical and economic barriers to installation and operation. While studies of the diagnostic performance of prostate MRI at 0.55T are needed for acceptance in imaging guidelines, our initial volunteer T2 and diffusion images at 0.55T presented here demonstrate adequate spatial and functional resolution for diagnostic use, with quality approaching that of images at 1.5T and 3T. Similarly, the isotropic 3D T2-weighted images and quantitative MRI thermometry mapping sequences specific to TULSA were demonstrated to be adequate to plan and control prostate ablation at 0.55T. For interventional radiology or urology practices with a prostate focus, MAGNETOM Free.Max presents a unique opportunity to reduce the cost and complexity of offering high-quality prostate MRI for a more efficient patient pathway that uses MRI for prostate cancer screening, detection, biopsy targeting, surveillance, in-bore interventions such as TULSA, and follow-up.

References

1 Drost F-JH, Osses D, Nieboer D, Bangma CH, Steyerberg EW, Roobol MJ, et al. Prostate magnetic resonance imaging, with or without magnetic resonance imaging-targeted biopsy, and systematic biopsy for detecting prostate cancer: A Cochrane systematic review and meta-analysis. Eur Urol [Internet]. 2020;77(1):78–94. Available from: http://dx.doi.org/10.1016/j.eururo.2019.06.023

2 Englman C, Adebusoye B, Maffei D, Stavrinides V, Bridge J, Kirkham A, et al. Magnetic resonance imaging-led risk-adapted active surveillance for prostate cancer: Updated results from a large cohort study. Eur Urol [Internet]. 2025;88(2):167–75. Available from: http://dx.doi.org/10.1016/j.eururo.2025.03.019

3 Giganti F, Dickinson L, Orczyk C, Haider A, Freeman A, Emberton M, et al. Prostate Imaging after Focal Ablation (PI-FAB): A proposal for a scoring system for multiparametric MRI of the prostate after focal therapy. Eur Urol Oncol [Internet]. 2023;6(6):629–34. Available from: http://dx.doi.org/10.1016/j.euo.2023.04.007

4 Light A, Mayor N, Cullen E, Kirkham A, Padhani AR, Arya M, et al. The Transatlantic Recommendations for Prostate Gland Evaluation with magnetic resonance imaging after Focal Therapy (TARGET): A systematic review and international consensus recommendations. Eur Urol [Internet]. 2024;85(5):466–82. Available from: http://dx.doi.org/10.1016/j.eururo.2024.02.001

5 Panebianco V, Villeirs G, Weinreb JC, Turkbey BI, Margolis DJ, Richenberg J, et al. Prostate magnetic resonance imaging for local Recurrence Reporting (PI-RR): International consensus -based guidelines on multiparametric magnetic resonance imaging for prostate cancer recurrence after radiation therapy and radical prostatectomy. Eur Urol Oncol [Internet]. 2021;4(6):868–76. Available from: http://dx.doi.org/10.1016/j.euo.2021.01.003

6 Thorley N, Parry T, Giganti F, Kopcke D, Sidhu HS, Brembilla G, et al. Diagnostic accuracy of abbreviated biparametric MRI for prostate cancer screening: a prospective feasibility study (ReIMAGINE study). Eur Radiol [Internet]. 2026;36(3):1959–70. Available from: http://dx.doi.org/10.1007/s00330-025-11837-1

7 Busch JJ Jr. The role for MRI-guided transurethral ultrasound ablation in the continuum of prostate cancer care. Br J Radiol [Internet]. 2022;95(1131):20210959. Available from: http://dx.doi.org/10.1259/bjr.20210959

8 Sprenkle PC, Seibert TM, Moses KA, Bahler C, Box G, Catalona WJ, et al. NCCN Guidelines [Internet]. NCCN Clinical Practice Guidelines in Oncology: Prostate Cancer Early Detection. 2026 [cited 2026 Sept 7]. Available from: https://www.nccn.org/guidelines/guidelines-detail?category=2&id=1460

9 Westphalen AC, McCulloch CE, Anaokar JM, Arora S, Barashi NS, Barentsz JO, et al. Variability of the positive predictive value of PI-RADS for prostate MRI across 26 centers: Experience of the Society of Abdominal Radiology Prostate Cancer Disease-focused Panel. Radiology [Internet]. 2020;296(1):76–84. Available from: http://dx.doi.org/10.1148/radiol.2020190646

10 Giganti F, Ng A, Asif A, Chan VW-S, Rossiter M, Nathan A, et al. Global variation in magnetic resonance imaging quality of the prostate. Radiology [Internet]. 2023;309(1):e231130. Available from: http://dx.doi.org/10.1148/radiol.231130

11 Purysko AS, Zacharias-Andrews K, Tomkins KG, Turkbey IB, Giganti F, Bhargavan-Chatfield M, et al. Improving prostate MR image quality in practice-initial results from the ACR prostate MR Image Quality Improvement Collaborative. J Am Coll Radiol [Internet]. 2024;21(9):1464–74. Available from: http://dx.doi.org/10.1016/j.jacr.2024.04.008

12 Bird VY, Masihy K, Varela J, Busch J. Correlation of MRI-derived apparent diffusion coefficient (ADC) values with Gleason scores in prostate cancer and quantitative prostate MRI reading. Cureus [Internet]. 2026;18(4):e106336. Available from: http://dx.doi.org/10.7759/cureus.106336

13 Ng ABCD, Asif A, Agarwal R, Panebianco V, Girometti R, Ghai S, et al. Biparametric vs multiparametric MRI for prostate cancer diagnosis: The PRIME diagnostic clinical trial: The PRIME diagnostic clinical trial. JAMA [Internet]. 2025;334(13):1170–9. Available from: http://dx.doi.org/10.1001/jama.2025.13722

14 Belue MJ, Law YM, Marko J, Turkbey E, Malayeri A, Yilmaz EC, et al. Deep learning-based interpretable AI for prostate T2W MRI quality evaluation. Acad Radiol [Internet]. 2024;31(4):1429–37. Available from: http://dx.doi.org/10.1016/j.acra.2023.09.030

15 Leapman MS, Dinan M, Pasha S, Long J, Washington SL 3rd, Ma X, et al. Mediators of racial disparity in the use of prostate magnetic resonance imaging among patients with prostate cancer. JAMA Oncol [Internet]. 2022;8(5):687–96. Available from: http://dx.doi.org/10.1001/jamaoncol.2021.8116

16 Lemberskiy G, Chandarana H, Bruno M, Ginocchio LA, Huang C, Tong A, et al. Feasibility of accelerated prostate diffusion-weighted imaging on 0.55 T MRI enabled with random matrix theory denoising. Invest Radiol [Internet]. 2023;58(10):720–9. Available from: http://dx.doi.org/10.1097/RLI.0000000000000979

17 Segeroth M, Breit H-C, Wasserthal J, Bach M, Rentsch C, Matthias M, et al. AI-based evaluation of prostate MR imaging at a modern low-field 0.55 T scanner compared to 3 T in a screening cohort. Acad Radiol [Internet]. 2025;32(5):2700–6. Available from: http://dx.doi.org/10.1016/j.acra.2024.11.024

18 Kaur T, Jiang Y, Seiberlich N, Hussain H, Wells S, Wei J, et al. Clinical feasibility of MRI-guided in-bore prostate biopsies at 0.55T. Abdom Radiol (NY) [Internet]. 2025;50(8):3773–83. Available from: http://dx.doi.org/10.1007/s00261-024-04783-x

19 Chopra R, Colquhoun A, Burtnyk M, N'djin WA, Kobelevskiy I, Boyes A, et al. MR imaging-controlled transurethral ultrasound therapy for conformal treatment of prostate tissue: initial feasibility in humans. Radiology [Internet]. 2012;265(1):303–13. Available from: http://dx.doi.org/10.1148/radiol.12112263

20 Ramsay E, Mougenot C, Staruch R, Boyes A, Kazem M, Bronskill M, et al. Evaluation of focal ablation of magnetic resonance imaging defined prostate cancer using magnetic resonance imaging controlled transurethral ultrasound therapy with prostatectomy as the reference standard. J Urol [Internet]. 2017;197(1):255–61. Available from: http://dx.doi.org/10.1016/j.juro.2016.06.100

21 Chin JL, Billia M, Relle J, Roethke MC, Popeneciu IV, Kuru TH, et al. Magnetic resonance imaging-guided transurethral ultrasound ablation of prostate tissue in patients with localized prostate cancer: A prospective phase 1 clinical trial. Eur Urol [Internet]. 2016;70(3):447–55. Available from: http://dx.doi.org/10.1016/j.eururo.2015.12.029

22 Klotz L, Pavlovich CP, Chin J, Hatiboglu G, Koch M, Penson D, et al. Magnetic resonance imaging-guided transurethral ultrasound ablation of prostate cancer. J Urol [Internet]. 2021;205(3):769–79. Available from: http://dx.doi.org/10.1097/JU.0000000000001362

23 Eggener S, Zagaja G, Oto A, Pavlovich C, Macura K, Koch M, et al. Pivotal study of MRI-guided transurethral ultrasound ablation (Tulsa) of localized prostate cancer: 5-year follow up. Urol Oncol [Internet]. 2024;42:S83. Available from: http://dx.doi.org/10.1016/j.urolonc.2024.01.234

24 Anttinen M, Mäkelä P, Nurminen P, Pärssinen H, Malaspina S, Sainio T, et al. Salvage magnetic resonance imaging-guided transurethral ultrasound ablation for localized radiorecurrent prostate cancer. Eur Urol Open Sci [Internet]. 2025;71:69–77. Available from: http://dx.doi.org/10.1016/j.euros.2024.11.001

25 Viitala A, Anttinen M, Mäkelä P, Pärssinen H, Nurminen P, Sainio T, et al. Magnetic resonance imaging-guided transurethral ultrasound ablation for benign prostatic obstruction: 1-year clinical outcomes of a phase II study. BJU Int [Internet]. 2025;136(3):473–83. Available from: http://dx.doi.org/10.1111/bju.16795

26 Woodrum D, Mynderse L, Raman S, Sella D, Frey G, Ghanouni P, et al. Abstract no. 50 randomized controlled trial of MRI-guided transurethral ultrasound ablation (TULSA) versus robotic prostatectomy for intermediate-risk prostate cancer: Ablation parameters and initial perioperative outcomes. J Vasc Interv Radiol [Internet]. 2026;37(4):108057. Available from: http://dx.doi.org/10.1016/j.jvir.2026.108057

27 Bird V, Busch K, Rose R, Varela J, Busch J. Prostate cancer treatment in the extreme apex: Preservation of continence with robotic-assisted MRI-guided transurethral ultrasound ablation. Cureus [Internet]. 2026;18(5):e108671. Available from: http://dx.doi.org/10.7759/cureus.108671

Contact

Joseph J. Busch, Jr., M.D.
Oncological Radiologist
Busch Center
Brookside Concourse 100
3650 Brookside Pkwy, Suite 175
Alpharetta, GA 30022
USA
Tel.: +1 770-424-6270
contacts@buschcenter.com
https://buschcenter.com